J Solid State Electrochem (2011) 15:1063–1070
DOI 10.1007/s10008-010-1275-6

ORIGINAL PAPER

Experimental and theoretical studies on the corrosion properties of some conducting polymer coatings

Rovshan Hasanov · Semra Bilgiç · Gökhan Gece

Received: 4 August 2010 / Revised: 6 December 2010 / Accepted: 7 December 2010 / Published online: 30 December 2010

Abstract In this study, the effects of poly(*N*-ethylaniline) (PNEA) monolayer coating and PPY/PNEA and PNEA/PPY bilayer coatings, which were formed on the low carbon steel (LCS) surface by electropolymerization in 0.1 M monomer + 0.3 M oxalic acid medium, on the corrosion of the LCS in 1 M H_2SO_4 medium have been investigated. LCS electrodes, which were coated with each of these conductive polymer layers, were held in 1 M H_2SO_4 medium for various time periods, in order to obtain current potential curves, and with the help of these curves, the corrosion parameters have been determined. Experimental findings show that the LCS coated with polymer layers prevent the corrosion of bare LCS in 1 M H_2SO_4 medium and bilayer PPY/PNEA and PNEA/PPY coatings are better than monolayer PNEA coating. In order to elucidate the interaction between the coatings and the metal, theoretical calculations have been done using AM1 semiempirical method. The calculated data have been found to support experimental findings.

Keywords Polymers · Coatings · Corrosion inhibition · Poly (*N*-ethylaniline)

Introduction

Corrosion inhibitors are widely used in industry to reduce the corrosion rate of metals and alloys in contact with aggressive environments. Most of the corrosion inhibitors are very hazardous to environments. Therefore, there is a rigorous search underway for an environmentally friendly alternative to be used in corrosion control. In this respect, electroactive conducting polymers are possible alternatives to toxic inhibitors [1–9]. The most frequently used polymers in corrosion prevention are polyaniline, polypyrrole, polythiophene, and polyacetylene [10–12]. Electropolymerization of monomers is typically carried out in acidic medium in order to enhance the solubility properties of monomers in aqueous solution and to keep the substrate surface in a passive state during electropolymerization process. Iroh group [13–15] studied in detail the electrochemical synthesis of polypyrrole (PPY) and poly(*N*-methylpyrrole) on mild steel substrates from oxalic acid solution. An adherent polymer film was easily formed on the substrate due to formation of iron salts on the surface in the active state of low carbon steel (LCS).

It is well known that monolayer conducting polymer coatings are more porous than bilayer ones, even electropolymerized from oxalic acid solution [16]. In our previous work [17], polyaniline (PANI) and polypyrrole, obtained by electropolymerization, were deposited on steel surface using cyclic voltammetric method and corrosion parameters were determined for various immersion time intervals in 1 M H_2SO_4. Moreover, the corrosion protection efficiencies of PPY/PANI- and PANI/PPY-coated steel determined for the same immersion time intervals in 1 M H_2SO_4, were compared with the corrosion protection efficiencies of monolayer coatings. It was shown that PPY/PANI and PANI/PPY bilayer conducting polymer coatings in 1 M H_2SO_4 were more effective than monolayer PPY and PANI coatings for the corrosion protection of steel.

In this study, however, poly(*N*-ethylaniline) (PNEA) conductive polymer was electrochemically synthesized by using *N*-ethylaniline monomer and steel electrode was coated with this polymer. The corrosion protection efficien-

R. Hasanov · S. Bilgiç (✉) · G. Gece
Department of Physical Chemistry, Faculty of Science,
Ankara University,
06100 Beşevler,
Ankara, Turkey
e-mail: bilgic@science.ankara.edu.tr

Table 1 Chemical composition (wt.%) of LCS used as electrode

C	Mn	Ni	P	S	Si	Cr	Cu	Fe
0.113	0.332	0.106	0.01	0.024	0.21	0.05	0.05	Remainder

cies of this monolayer coating, and PPY/PNEA and PNEA/PPY bilayer coatings in 1 M H_2SO_4 medium were investigated. Experimental results were further supported by using quantum mechanical calculations. It has been well established in the literature that theoretical approaches provide means for clarification of interactions between molecules and metal surfaces, and recently, some theoretical studies on small oligomers have been used to predict the inhibition effects [18, 19]. Thus, calculations on reduced (RD-PNEA) and oxidized (OD-PNEA) dimers were also performed to elucidate the inhibition behavior of PNEA by using the semiempirical AM1 method [20].

Experimental

Materials and methods

All chemicals used in this study were pure at analytical grade purchased from Merck. The chemical composition of the LCS is given in Table 1. The LCS electrode preparation and treatment was described in our previous study [17]. Bi-distilled water was used for preparing the solutions and to remove excess reactant from the coated LCS. The emery paper was not used to treat the electrode after the electrosynthesis of polymer coatings. All tests, such as electropolymerization and corrosion tests were carried out in a three-electrode cell. The steel electrode was placed in the center of the cell, and SCE and platinum plate in other parts of cell were used as reference and counter electrode, respectively. All potentials obtained in this study were measured with respect to SCE. Before each experiment, nitrogen gas was passed through the solutions for up to 20 min in order to remove dissolved oxygen. The experiments were carried out using the system consisting of Wenking LB 75L Laboratory model potentiometer, Wenking VSG72 model voltage scanning generator, Yokogawa Technicorder Type 3077 recorder, BM 101 thermostat, and Electromag mixer. In order to determine the corrosion parameters, Tafel extrapolation method was used. Electro-

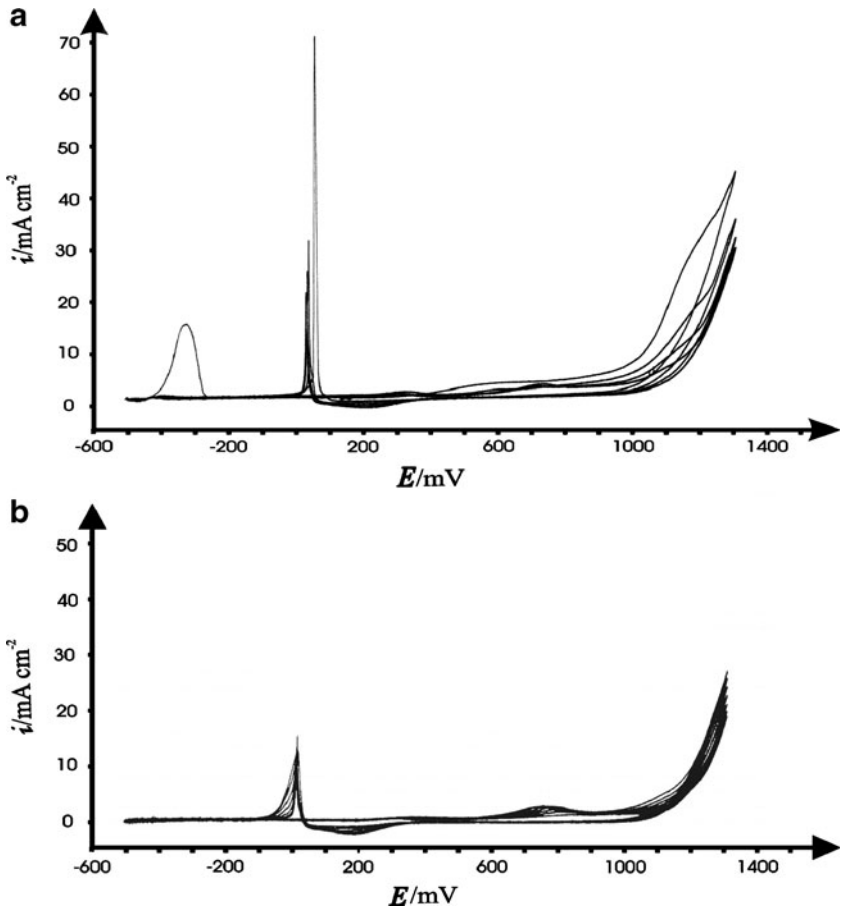

Fig. 1 **a** The initial four cycles and **b** fifth to 11th cycles of the voltammogram for the electrochemical synthesis of PNEA on LCS

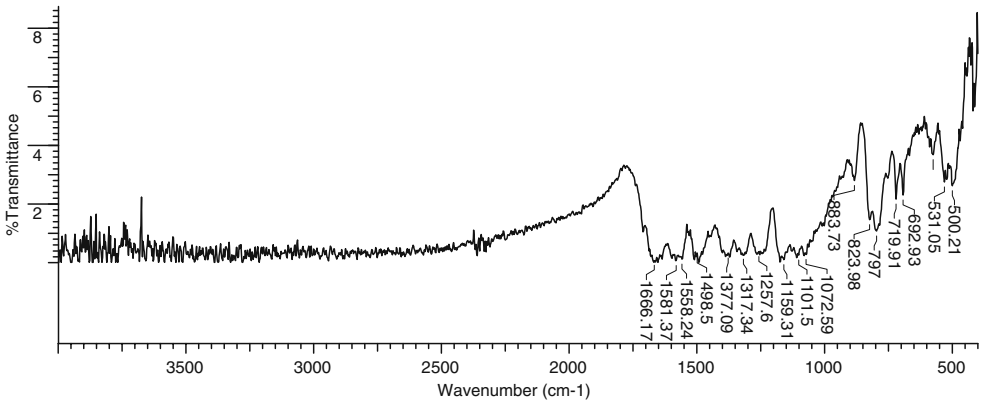

Fig. 2 FTIR spectrum for PNEA

chemical corrosion measurements were performed in 1 M H_2SO_4 solution at room temperature. 0.3 M, oxalic acid, and 0.1 M PY solution were used to coat the bare and PNEA-coated LCS with PPY film. To obtain the PNEA coatings, 0.3 M oxalic acid and 0.1 M NEA were used during electropolymerization to coat both the bare and PPY-coated LCS. Potential scan rate was 2.5 mV s^{-1} until the formation of $Fe_2C_2O_4$ on the LCS surface. Afterwards, in order to obtain a compact monolayer coating, a 50 mV s^{-1} scan rate was applied until the end of electropolymerization. The scan rate was set at 50 mV s^{-1} in order to form a bilayer coating on the LCS surface. The chemical structure of the coatings formed by electrochemical polymerization was characterized using Fourier transform infrared (FTIR) spectroscopy. FTIR spectra of the coatings in KBR pellets were recorded in a transmission mode using EQUINOX 55 FTIR spectrometer (Bruker, resolution 30). The spectra were collected in the 4,000–500 cm^{-1} range.

Computational details

All calculations were carried out using HyperChem program [21]. The reduced (RD-PNEA) and oxidized PNEA (OD-PNEA) dimers were individually optimized using the AM1 semiempirical method. The convergence limit for the optimization was 1.0 kcal$Å^{-1}$ mol^{-1}, with the use of the Polak-Ribiere conjugate gradient algorithm [22]. The electronic properties such as highest occupied molecular orbital (E_{HOMO}) energy, lowest unoccupied molecular orbital (E_{LUMO}) energy, and the energy gap ($\Delta E = E_L - E_H$) have been calculated.

Results and discussion

Electrochemical synthesis of PNEA coating

The initial fourth and fifth to 11th cycles of cyclic voltammogram of PNEA electrodeposition are shown in Fig. 1a and b, respectively. The electrosynthesis was carried out on the LCS in aqueous solution containing 0.3 M oxalic acid and 0.1 M NEA using cyclic voltammetry. It is clearly seen from Fig. 1a that E_{ocp} in this medium was about −500 mV. Scan range was set to 1,800 mV. The scan rate was set to 2.5 mV s^{-1} at the potentials starting from E_{ocp} up to −250 mV. The formation of $Fe_2C_2O_4$ occurred in this potential range. The scan rate was set at 50 mV s^{-1}, in order to obtain a well-formed PNEA coating on the surface of LCS in the passive region. It may be understood from the first cycle of this voltammogram that the first monomer radical cation appeared at 500 mV, but subsequent generation of participation reaction during the

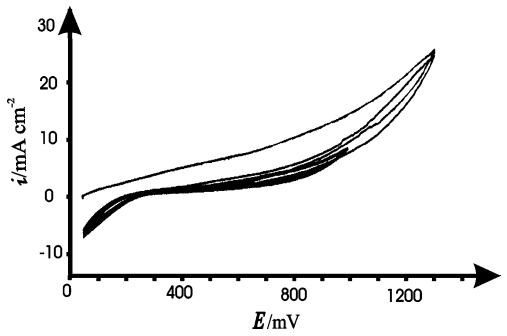

Fig. 3 The initial fourth cycles of the voltammogram for the electrochemical synthesis of PPY/PNEA on LCS (scan rate=50 mV s^{-1})

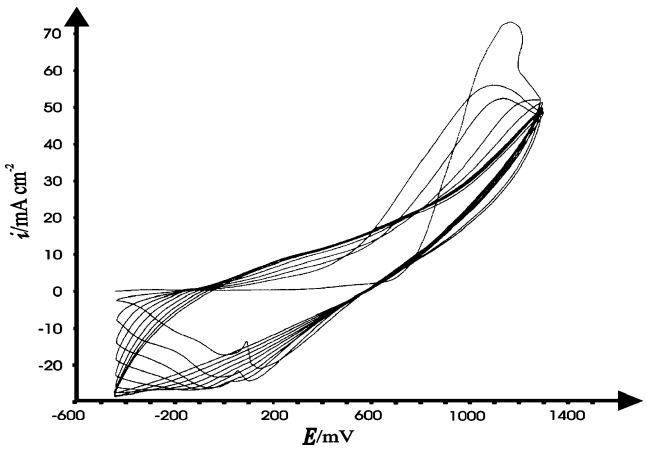

Fig. 4 Initial 15th cycles of the voltammogram for the electrochemical synthesis of PNEA/PPY on LCS (scan rate=50 mV s^{-1})

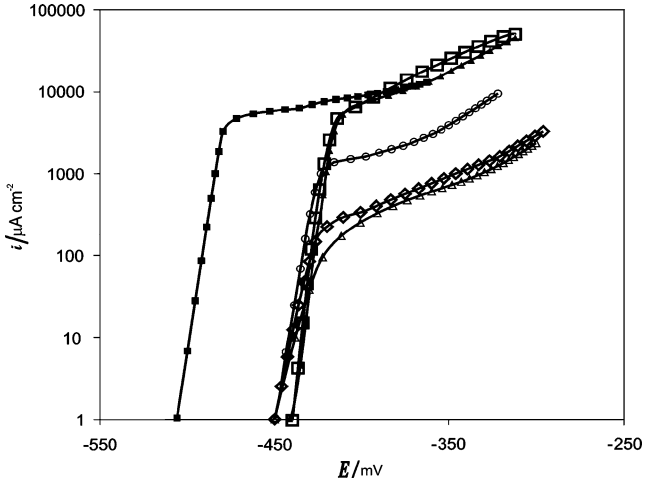

Fig. 5 The anodic Tafel curves for (*close square*) bare and PNEA-coated LCS (*open triangle*) without immersion time and with (*open diamond*) 10 min, (*open circle*) 50 min, (*close triangle*) 100 min, and (*open square*) 180 min of immersion time in 1 M H_2SO_4

second and third cycles occurred at 600 and 700 mV, respectively. In the backward scan, a repassivation peak could be seen at about 70 mV in the first cycle, and for subsequent cycles it is observed that the potentials were slightly different from those in the first cycle. The values were 40, 30, and 20 mV, and the intensities of repassivation peaks were lower than that those in the first cycle. In the backward scan, the potentials of reduction part of monomer participation reaction were almost equal to 200 mV, considering both Fig. 1a and b.

FTIR analysis

In Fig. 2, the characteristic IR peaks observed at 1,581, 1,498, 1,377, 1,258, 1,102, and 575 cm^{-1} correspond to the emeraldine form of PNEA which are attributed to the vibration modes of quinoid and benzenoid rings, the imine structure, and in-plane and out-of-plane CH bending modes of benzenoid groups of the emeraldine PNEA film [23]. The peak at 823 cm^{-1} is due to 1,4-para-disubstituted benzene ring, which is expected for the PNEA structure. It may be explained by the fact that PNEA is in the form of emeraldine base during in situ polymerization in 0.3 M oxalic acid solution containing 0.1 M NEA. Other peaks at 1,666, 1,317, and 1,159 cm^{-1} were attributed to C=O and C–O stretches, respectively, due to FeC_2O_4 formation on the steel, while 1,558, 1,072, 883, 797, 720, 693, 531, and 500 cm^{-1} were most probably related to the interception of dopant ions in the polymer matrix.

Synthesis of the top coating on the primer-coated LCS

There are few studies related to the inhibitive effects of double-layer conductive polymer coatings on steel corrosion in acidic medium [17, 24]. In this study, bilayer coatings were formed by the synthesis of top coatings on the primer-coated LCS.

PPY/PNEA coating synthesis

PPY was coated on the LCS electrode in 0.1 M PY and 0.3 M oxalic acid solution. The scan rate was set to 2.5 mV s^{-1} in order to get a well-distributed FeC_2O_4 in the active region of the LCS. In order to form strongly adherent and homogeneous polymer layers on the surface, the scan rate was set to 50 mV s^{-1}. After that, the PPY-coated electrode was placed in 0.3 M oxalic acid containing 0.1 M NEA in order to be top coated by PNEA (Fig. 3). PNEA formed under such conditions is in oxidized form. The start potential of PPY-coated electrode in the 0.3 M oxalic acid solution containing 0.1 M NEA was 60 mV. The scan range was 1,200 mV, so that the scan was made up to 1,320 mV and then backwards. It can be seen from Fig. 3 that the electrode is passive in this potential range, and no activation peak is observed during electropolymerization of PPY/PNEA on the LCS surface. During the first cycle at 1,000 mV, the passed current density was 15 mA cm^{-2} and after two cycles it dropped down to the values of 11 and 8 mA cm^{-2}, respectively, suggesting that the rate of the top film growth on the primer coating decreased after each cycle.

PNEA/PPY coating synthesis

The PNEA/PPY coatings on the LCS surface were successfully obtained by electropolymerization employing PNEA-

Table 2 Tafel parameters for bare and PNEA-coated LCS after immersion in 1 M H_2SO_4

Electrode	Immersion time (min)	$-E_{corr}$ (mV)	b_a (mV)	i_{corr} (μA/cm²)	η%
Bare LCS	–	505	112	3,930	–
LCS/PNEA	0	450	70	70	98.2
	10	450	100	100	97.5
	50	450	116	500	87.3
	100	440	100	2,190	44.3
	150	440	107	2,600	33.8
	180	440	105	3,100	21.1

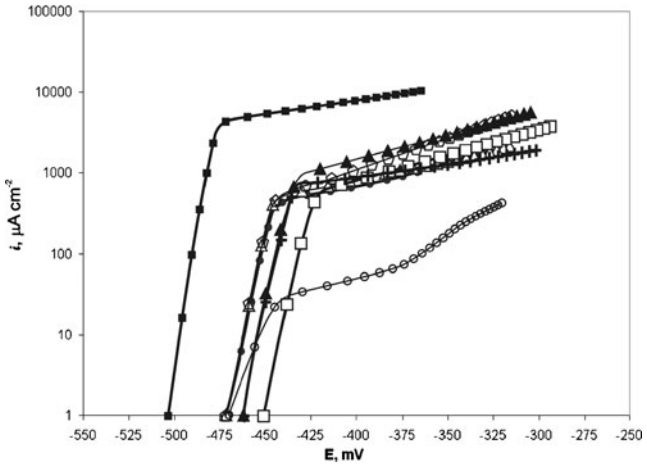

Fig. 6 The anodic Tafel curves for (*close square*) bare and PPY/PNEA-coated LCS (*open circle*) without immersion time and with (⬠) 10 min, (*close circle*) 50 min, (*open triangle*) 100 min, (*close triangle*) 150 min, (*open square*) 210 min, and (*plus sign*) 300 min of immersion time in 1 M H_2SO_4

coated steel in 0.3 M oxalic acid solution containing 0.1 M PY (Fig. 4). Polymerization was confirmed by 15 successful cycles seen in Fig. 4. In this medium E_{ocp} was −460 mV and the scan range and the scan rate was set to 1,760 mV and 50 mV s^{-1}, respectively. The activation peak was not observed during double-layer electropolymerization. The monomer oxidation commenced at approximately 700 mV, and the peak current density passed in this cycle was nearly 73 mA cm^{-2}. The current densities in subsequent cycles were lower than in first cycle which may be explained by decreasing rate of polymer formation with the number of cycles. The reactivation peak was observed at 100 mV in the backward scan of the first cycle, the intensities of these peaks decreased at subsequent cycles. No reactivation peak was observed after five cycles.

Corrosion tests

The corrosion tests for bare steel and PPY-, PNEA-, PPY/PNEA-, and PNEA/PPY-coated LCS were carried out in 1 M H_2SO_4 solution. The percentage inhibition efficiency, η%, and the surface coverage, θ, were calculated from the following equations:

$$\eta\% = \left(\frac{i_0 - i_1}{i_0}\right) \cdot 100 \quad (1)$$

$$\theta = \frac{i_0 - i_1}{i_0} \quad (2)$$

where i_0 and i_1 are the corrosion current densities without and with inhibitor.

PNEA coating

The anodic Tafel curves for PNEA-coated steel in 1 M H_2SO_4 solution are shown in Fig. 5 and the corrosion parameters obtained for this electrode are shown in Table 2. As compared to PPY, the PNEA coating was found to be an anodic coating in this solution and the electrode potential was found to be −450 mV. After increasing the immersion time in corrosive medium, the potentials shifted to more positive values and this observation indicated that PNEA coating functioned as an anodic coating. The PPY coating showed a corrosion efficiency of 46.6% after 180 min of immersion in 1 M H_2SO_4, but the corrosion efficiency of PNEA coating (21.1%) was much lower than that of PPY coating. Meanwhile, there was no agreement between anodic Tafel constants.

PPY/PNEA coating

PPY/PNEA-coated LCS was tested in 1 M H_2SO_4 solution and the results obtained were compared with that for monolayer-coated LCS. The anodic Tafel curves are shown in Fig. 6. After initial observation, it was evident that this bilayer coating functioned as anodic coating due to the electrode potentials found at more positive potentials. The corrosion potential of PPY/PNEA-coated electrode fluctuated during immersion for 300 min in 1 M H_2SO_4. In order to compare the corrosion current densities, the corrosion efficiencies were calculated by using Eq. 1. It is quite clear

Table 3 Tafel parameters for bare and PPY/PNEA-coated LCS after immersion in 1 M H_2SO_4

Electrode	Immersion time (min)	$-E_{corr}$ (mV)	b_a (mV)	i_{corr} (μA/cm^2)	η%
Bare LCS	–	505	112	3,930	–
LCS/PPY/PNEA	0	500	177	20	99.5
	10	470	119	260	93.4
	50	470	205	280	92.9
	100	470	226	350	91.1
	150	450	155	290	92.6
	210	460	350	500	87.3
	300	470	119	260	93.4

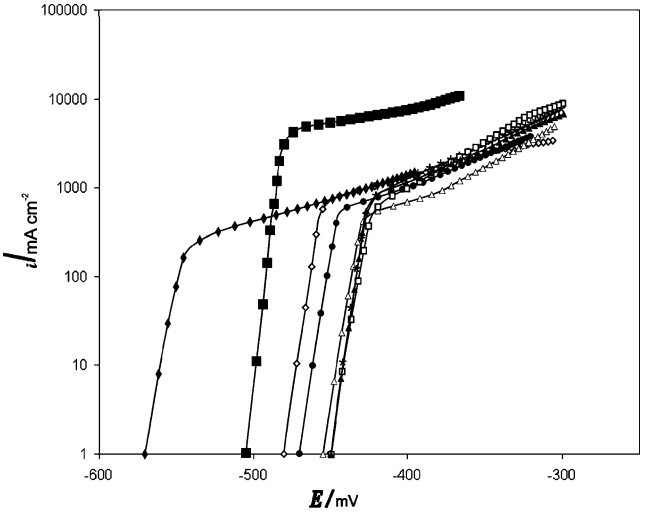

Fig. 7 The anodic Tafel curves for (*close square*) bare and PNEA/PPY-coated LCS (*close diamond*) without immersion time and with (*open diamond*) 10 min, (*close circle*) 50 min, (*open triangle*) 100 min, (*close triangle*) 150 min, (*) 200 min, and (*open square*) 270 min of immersion in 1 M H_2SO_4

from Table 3 that there is a steady-state between the rates of electrode corrosion and repassivation in this corrosive medium. In other words, the efficiency values also fluctuated with immersion time in corrosive medium. The lowest corrosion efficiency observed during immersion for 300 min was 87.3%. This observation is explained below in terms of the most suitable proposed mechanism.

PNEA/PPY coating

The anodic Tafel curves of PNEA/PPY coating in 1 M H_2SO_4 are shown in Fig. 7 and the corrosion parameters obtained from these curves are given in Table 4. After a 10-min immersion of the PNEA/PPY-coated steel in 1 M H_2SO_4 solution, the electrode potential was found to be −570 mV suggesting a cathodic inhibition. However, a positive shift to −480 mV was further observed after immersion for 10 min. The corrosion potential changed to −450 mV after subsequent immersion for up to 270 min in acidic medium. Corrosion current densities for the PNEA/PPY-coated LCS as a function of immersion time were much lower than those for bare, PPY- and PNEA-coated LCS. However, the performance of the PPY/PNEA coating remained constant with immersion time in the corrosive medium.

Protective mechanism of conducting polymer coating on the surface of LCS

Protection by PPY/PNEA and PNEA/PPY coatings doped with oxalate ions was better than by PNEA monolayer as seen in Tables 2–4. Bare LCS was unprotected in 1 M H_2SO_4 solution and the formed oxide films which occurred in the surface of LCS had no protection features to keep corrosion rate slow enough. Therefore, the application of double-layer conducting polymers which have unexpected attributes when doped with dopants (i.e., oxalate ions which enhance solubility properties of monomer in aqueous solution) was taken into consideration in this study. Although defects have important effects for such coatings, these effects are only considered in a few studies [25].

The protection mechanism of double-layer conducting polymers depends mostly on dopants used in electrosynthesis. It is a considerable expectation that the dopant anions form insoluble salts with major components of LCS in corrosive medium at potentials which LCS is unprotected. In order to prevent the corrosive agents reaching the surface of LCS, the physical barrier is another property which has additional effect on protection. Su and Iroh [15] claimed that $FeC_2O_4{\cdot}2\ H_20$ forms during Fe/Fe^{2+} oxidation in the active potential region in the cyclic voltammograms of LCS in the presence of oxalate ions. This salt is not stable as other salts of iron, and Fe exists as Fe^{2+} up to 800 mV and as Fe^{3+} at subsequent potentials. For this reason, at substantial potentials of voltammograms of LCS, Fe^{2+} will turn into Fe^{3+} and will form $Fe_2(C_2O_4)_3$, which is still a good soluble salt in the aquatic solution. Meanwhile monomer oxidation will start on the surface at the potentials around which Fe^{2+} turns into Fe^{3+}. Su and Iroh [15] also affirmed that the passiveness gained by FeC_2O_4 was lower than that gained by conductive polymer. Our findings are in well accordance with these authors.

Table 4 Tafel parameters for bare and PNEA/PPY-coated LCS after immersion in 1 M H_2SO_4

Electrode	Immersion time (min)	$-E_{corr}$ (mV)	b_a (mV)	i_{corr} (μA/cm^2)	η%
Bare LCS	–	505	112	3,930	–
LCS/PNEA/PPY	0	570	278	200	94.9
	10	480	207	500	87.3
	50	470	135	300	92.4
	100	455	131	250	93.6
	150	450	125	420	89.3
	200	450	125	450	88.5
	270	450	88	250	93.6

Table 5 Energies of the frontier orbitals and energy gaps (ΔE) for the interaction of RD-PNEA, OD-PNEA, and iron

	E_{HOMO} (eV)	E_{LUMO} (eV)	ΔE (eV)	
RD-PNEA	−7.626	0.531	8.341[a]	7.376[b]
OD-RNEA	−4.102	0.187	7.997[c]	3.852[d]
Fe	−7.81	−0.25		

[a] $E_{LUMO\ RD\text{-}PNEA}-E_{HOMO\ Fe}$

[b] $E_{LUMO\ Fe}-E_{HOMO\ RD\text{-}PNEA}$

[c] $E_{LUMO\ OD\text{-}PNEA}-E_{HOMO\ Fe}$

[d] $E_{LUMO\ Fe}-E_{HOMO\ OD\text{-}PNEA}$

Quantum chemical study

There are certain quantum chemical parameters that can be related to the metal–molecule interactions [26]. Among these, we can mention the energy of the highest molecular orbital that is often associated with the capacity of a molecule to donate electrons. Hence, an increase in the values of E_{HOMO} can facilitate the adsorption and therefore the inhibition efficiency, by indicating the disposition of the molecule to donate orbital electrons to an appropriate acceptor with empty molecular orbitals. In the same way, low values of the energy gap ($\Delta E=E_{LUMO}-E_{HOMO}$) will render good inhibition efficiencies, because the energy needed to remove an electron from the last occupied orbital will be low.

The energies of HOMO and LUMO were calculated for reduced poly(*N*-ethylaniline) and oxidized poly(*N*-ethylaniline) dimers using AM1 method (Table 5) and frontier orbital densities are shown in Fig. 8. For RD-PNEA, HOMO is distributed over opposite benzene rings which reasonably lowers the value of HOMO energy, and LUMO is mainly localized on the nitrogen atoms. Comparably, LUMO electron densities of OD-PNEA are confined on one side of the rings. On the other hand, the HOMO densities of OD-PNEA are located throughout the opposite benzene ring. E_{HOMO} and E_{LUMO} values for iron were taken as ionization potential and electron affinity, respectively [27]. As can be seen from Table 5, the interaction between the HOMO of RD-PNEA molecule and LUMO of metal atom is weaker than that between the HOMO of OD-PNEA molecule and the LUMO of metal atom. This observation points out that the interaction between OD-PNEA dimer and iron should be primarily the result of the interaction between the HOMO of OD-PNEA molecule and the LUMO of iron, that is, when adsorbing on steel surface, the OD-PNEA molecules act as electron pair donors.

Conclusions

The following results can be drawn from this study:

1. It has been found that bilayer conducting polymers (PPY/PNEA and PNEA/PPY) coatings on the steel surface in 1 M H_2SO_4 are more efficient than monolayer (PNEA) coating under same conditions.
2. Theoretical calculations show that oxidized forms of PNEA dimers act as electron donors when they

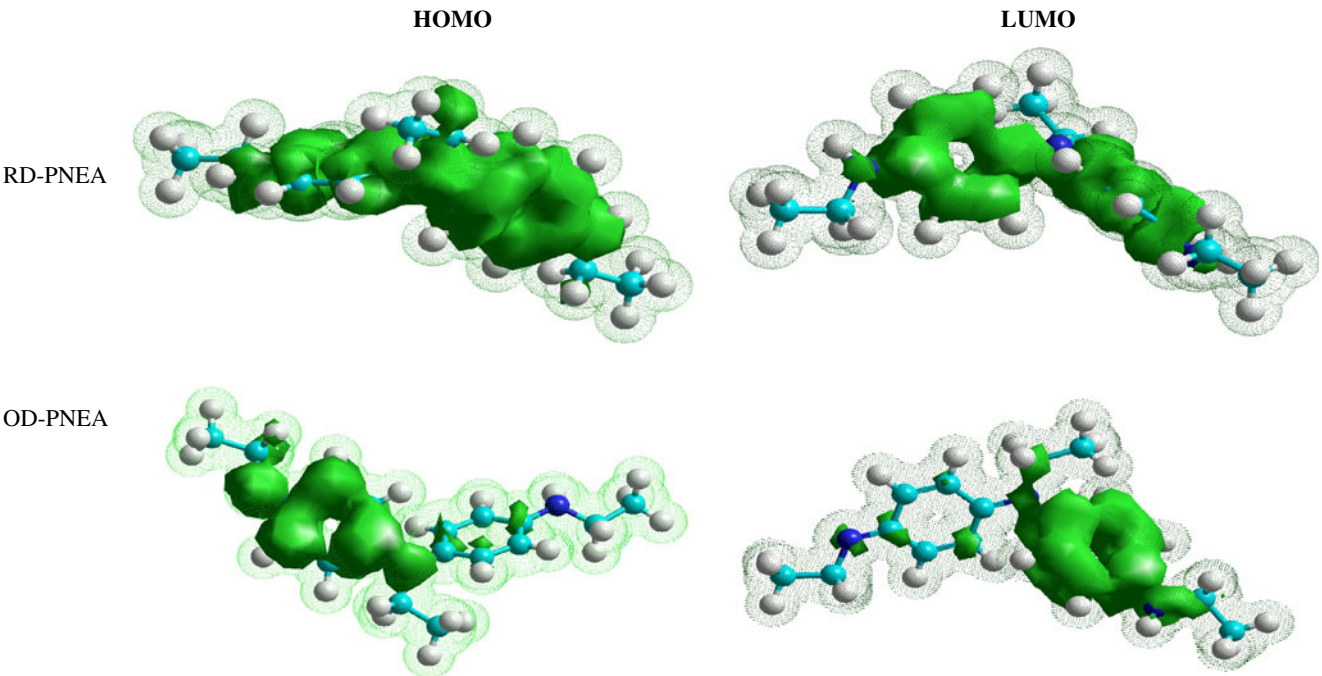

Fig. 8 The HOMO and LUMO densities for RD-PNEA and OD-PNEA dimers

interact with the steel surface and this seems to be the essential electronic mechanism forcing the interaction between the OD-PNEA molecule and the metal surface.

Acknowledgment The authors are indebted to The Scientific and Technical Research Council of Turkey (TUBITAK) for the scholarship (2215—Ph.D. Fellowship For Foreign Country Citizens) granted to Rovshan Hasanov.

References

1. Tallman DE, Spinks G, Dominis A, Wallace GG (2002) J Solid State Electrochem 6:73–84
2. Spinks GM, Dominis AJ, Wallace GG, Tallman DE (2002) J Solid State Electrochem 6:85–100
3. Tüken T, Yazıcı B, Erbil M (2006) Surf Coat Technol 200:4802–4809
4. Tüken T, Düdükcü M, Yazıcı B, Erbil M (2004) Prog Org Coat 50:273–282
5. Gelling VJ, Wiesta MM, Tallman DE, Bierwagen GP, Wallace GG (2001) Prog Org Coat 43:149–157
6. Martins I, Reis TC, Bazzaoui M, Bazzaoui EA, Martins L (2004) Corros Sci 46:2361–2381
7. Armelin E, Meneguzzi Á, Ferreira CA, Alemán C (2009) Surf Coat Technol 203:3763–3769
8. Sørensen PA, Kiil S, Dam-Johansen K, Weinell CE (2009) J Coat Technol Res 6:135–176
9. Nguyen PT, Rammelt U, Plieth W (2003) J Solid State Electrochem 7:497–502
10. Hammache H, Makhloufi L, Saidani B (2003) Corros Sci 45:2031–2042
11. Yağan A, Pekmez NÖ, Yıldız A (2008) Electrochim Acta 53:2474–2482
12. Zarras P, Anderson N, Webber C, Irvin DJ, Irvin JA, Guenthner A, Stenger-Smith JD (2003) Radiat Phys Chem 68:387–394
13. Su W, Iroh JO (1999) Electrochim Acta 44:3321–3332
14. Iroh JO, Su W (2000) Electrochim Acta 46:15–24
15. Su W, Iroh JO (2000) Synth Met 114:225–234
16. Tan CK, Blackwood DJ (2003) Corros Sci 45:545–557
17. Hasanov R, Bilgiç S (2009) Prog Org Coat 64:435–445
18. Sein LT Jr, Wei Y, Jansen SA (2001) Comp Theor Polym Sci 11:83–88
19. Sein LT Jr, Wei Y, Jansen SA (2004) Synth Met 143:1–12
20. Dewar MJS, Zoebisch EG, Healy EF, Stewart JJP (1985) J Am Chem Soc 107:3902–3909
21. HyperChem (2002) Hypercube Inc, Gainesville
22. Polak E, Ribiere G (1969) Rev Fr Inf Rech Oper 16-R1:35–43
23. Shah K, Iroh J (2002) Synth Met 132:35–41
24. Popović MM, Grgur BN, Mišković-Stanković VB (2005) Prog Org Coat 52:359–365
25. Rohwerder M, Michalik A (2007) Electrochim Acta 53:1300–1313
26. Gece G (2008) Corros Sci 50:2981–2992
27. Mutombo P, Hackerman N (1998) Anti-Corros Methods Mater 45:413–418